Korean J. Chem. Eng., **30**(8), 1566-1570 (2013)
DOI: 10.1007/s11814-013-0082-z

Catalytic activity and characterization of V_2O_5/γ-Al_2O_3 for ammoxidation of *m*-xylene system

Yukwon Jeon*, Sung wook Row*, Altansukh Dorjgotov*, Sang Duek Lee, Kyeongseok Oh***,†, and Yong-Gun Shul*,†**

*Department of Chemical and Biomolecular Engineering, Yonsei University, 134, Shinchon-dong, Seodaemun-gu, Seoul 120-749, Korea
**Clean Energy Research Center, Korea Institute of Science and Technology, P. O. Box 131, Cheongryang, Seoul 130-650, Korea
***Department of Chemical and Environmental Technology, Inha Technical College, 100, Inha-ro, Incheon 402-752, Korea
(*Received 5 March 2013 • accepted 9 May 2013*)

Abstract−An ammoxidation of *m*-xylene was evaluated in a fixed-bed reactor using V_2O_5 on various oxides. Catalysts were prepared by wet impregnation method. At first, the loading of V_2O_5 was varied from 5 wt% to 20 wt% on γ-Al_2O_3 support to estimate the most effective amount of V_2O_5. Second, the effect of catalyst supports was examined at 10 wt% loading of V_2O_5. V_2O_5/TiO_2 and V_2O_5/SiO_2 catalysts were employed to compare the ammoxidation reaction with V_2O_5/γ-Al_2O_3. Most catalytic activity was observed when γ-Al_2O_3 was used as a support. Careful characterization was followed by physicochemical techniques, such as BET measurement, X-ray diffraction (XRD), Raman spectroscopy and temperature-programmed reduction (TPR). The results provided the clue that monolayer V_2O_5 was favorably dispersed on the surface of γ-Al_2O_3 up to 10 wt%, which led to the highest yield of isophthalonitrile (IPN).

Key words: Ammoxidation, *m*-Xylene, V_2O_5, γ-Al_2O_3

INTRODUCTION

Vanadium oxide (V_2O_5) has been widely used in various oxidation reaction processes. The industrial application of V_2O_5 is often found in selective oxidation, oxidative dehydrogenation, partial oxidation of methanol to formaldehyde, selective catalytic reduction of nitrogen oxides in the presence of organic substrates [1-3]. V_2O_5 is also a well-known catalyst, specifically, to obtain aromatic nitriles through ammoxidation reaction of hydrocarbons. As an example of aromatic nitriles, isophthalonitrile (IPN) can be produced by ammoxidation of *m*-xylene. IPN is a widely applicable intermediate for producing pharmaceuticals, paints, resins, fibers, dyestuffs and pesticides [4-8].

In an ammoxidation reaction, V_2O_5 is usually supported by single oxides because of its poor thermal and mechanical stability inappropriately resulting in fast catalyst deactivation and unwanted high combustion of organic molecules. Often selected are γ-Al_2O_3, TiO_2, SiO_2 and ZrO_2 as support materials. Regarded as an inert material, in general, the support for catalyst provides sufficient surface for metal and metal oxide dispersion and increases the number of active sites and also enhances the thermal and mechanical stability of catalyst even at high temperatures. Analyses of physical and chemical properties related to metal dispersion and electronic effect are becoming more important to understand catalyst activity [9-11].

Ito and Sano did a kinetic study of the gas-phase ammoxidation of xylene isomers over V_2O_5 catalyst and reported that xylene ammoxidation has a complicated reaction mechanism bearing consecutive reaction steps, where tolunitrile (TN) is considered as an intermediate [12]. While, a single step reaction was studied by liquid-phase ammoxidation of *m*-xylene to generate *m*-tolunitrile, also an intermediate [7]. However, rarely reported has been IPN production, as a target chemical, directly from gas-phase *m*-xylene ammoxidation.

In terms of support oxide for V_2O_5, diverse researches have studied, for instance, o-xylene ammoxidation using vanadium phosphorus oxides (bulk VPO only, VPO/Al_2O_3, VPO/Al_2O_3, VPO/TiO_2) [5], $VCrO_x/SiO_2$ [13], V_2O_5/TiO_2-ZrO_2 [14], V_2O_5/ZrO_2 [15] and $V_2O_5/(TiO_2$ or $Al_2O_3)$ [6,16]. The mechanism of ammoxidation reaction has been explored as well. Lee [6] reported that catalytic performance of V_2O_5/TiO_2 xerogel was different when a catalyst was prepared by a different method. The study emphasized the important role of interaction between V_2O_5 and TiO_2 [6]. Niwa et al. [16] used V_2O_5/Al_2O_3 for xylene ammoxidation. They reported that xylene is oxidized on V_2O_5, stabilized as methyl benzoate ion on Al_2O_3 and finally converted to disyanobenzene. Ammoxidation of *m*-xylene only was also presented in various patents [17-19] and literature [20-23]. Superior performance of V_2O_5 was reported when V_2O_5 is impregnated with support oxide in a form of monolayer dispersion compared with bulk phase or multilayer dispersion on support oxide [24-28]. The method of impregnation, solid-solid-wetting, grafting, and chemical vapor deposition, has been employed individually to obtain a monolayer of the vanadium. The reaction effect of synthetic method, monolayer and/or multilayer formation and chemical state was shown elsewhere [29,30].

WE explored the effect of V_2O_5 on IPN production directly from

†To whom correspondence should be addressed.
E-mail: shulyg@yonsei.ac.kr, kyeongseok.oh@inhatc.ac.kr

m-xylene ammoxidation. At first, the optimum amount of V_2O_5 loading was determined by varying V_2O_5 amount from 5 wt% to 20 wt% on γ-Al_2O_3 using impregnation method. The study then expanded to see the effect of support oxides by employing TiO_2 and SiO_2. An interaction study between V_2O_5 and support oxides was done by various techniques: BET, X-ray diffraction (XRD), Raman spectroscopy, and temperature-programmed reduction (TPR). The study includes implicative interpretation of monolayer V_2O_5 dispersion on γ-Al_2O_3.

EXPERIMENTAL

1. Catalyst Preparation

Catalysts were prepared by wet impregnation method. Purchased were V_2O_5 (Kanto chemical), γ-Al_2O_3 (Johnson Matthey Inc., 122 m^2/g), SiO_2 (Johnson Matthey Inc., 422 m^2/g) and TiO_2 (Degussa, 53 m^2/g). V_2O_5 is the main catalyst and the rest are used as support materials ground uniformly before impregnation process. In brief introduction of impregnation procedure, V_2O_5 was dissolved in a hot water with 2 M oxalic acid dehydrate (Kanto chemical, 99%) at 85 °C for 30 min. Consecutively, the solution was mixed with oxide supports at different ratio of V_2O_5 to oxides. The excess water was considered to evaporate solely at room temperature during stirring. The dried samples were then ground again and calcined at 500 °C for 4 hours. A furnace was heated with 5 °C/min in an open-air condition up to 500 °C. Catalysts were varied loading amounts of V_2O_5 to γ-Al_2O_3 (5 wt%, 10 wt%, 15 wt% and 20 wt%), but fixed to individual SiO_2 and TiO_2 at 10 wt% of V_2O_5.

2. Characterization

Micromeritics ASAP 2010 was used to analyze surface area, distribution of pore volume and pore diameter in nitrogen atmosphere occurred adsorption-desorption at 77 K. Before measurement, all the samples were degassed at 120 °C overnight. The mesopore size was calculated by employing the Barnett-Joyner-Halenda method to the desorption branch of the isotherm. Crystallography of catalyst was examined by X-ray diffraction (XRD) measurement using a Rigaku D/MAX-II, which was installed with a monochromated CuKα radiation source at a wavelength of 1.5406 Å operating at 30 kV and 30 mA. XRD was recorded at a scan rate of 5°/min from 5° to 80°.

For physicochemical analyses, Raman spectroscopy and temperature-programmed reduction (TPR) were employed. First, Raman spectroscopy was used to investigate the surface interaction between V_2O_5 and support oxides under ambient and dehydrated conditions with a JY LabRam HR fitted with a liquid-nitrogen cooled CCD detector. The spectra were collected under ambient conditions using the 514.5 nm line of an argon-ion laser. Second, TPR was performed in a quartz microreactor surrounded by a PID controlled electric furnace under H_2/Ar flow. To remove H_2O formed during reduction process, a silica gel trap was placed and H_2 consumption was determined by a thermal conductivity detector.

3. Catalytic Activity

Catalytic reaction was performed in a fixed-bed tubular reactor (12 mm i.d.). Each experiment used 0.1 g of catalyst placed on quartz wool. Reaction pressure was set at atmosphere and heat tracer was installed to 200 °C along the production lines in order to prevent the solidification of main product, IPN, of which melting temperature is 168 °C. Reaction temperature was controlled in the range of 300-420 °C for 2-4 h according to the individual reaction condition. Mass flow controllers were used to control the mixture gases ratio *m*-xylene: NH_3 : O_2=1 (6.5 mg/h): 11 (3.5 mL/min): 5.4 (9 mL/min) from separate cylinders with *m*-xylene fed from a N_2-derived saturator at 10 °C. Products were analyzed by both gas chromatography (GC) and liquid chromatography (LC). While GC was mainly used to assay *m*-xylene, LC was used to analyze IPN and TN using a UV detector at 240 nm. Selected columns were installed: DB-5 in GC and Eclipse XDE-C8 in LC. During LC measurement, methanol was used as a mobile phase (1 mL/min) and the machine controlled the run time of 5 min. Conversion of *m*-xylene and yields of IPN/TN were calculated by using the following formulae below. Observed were CO+CO_2 yields of 3.4-5.7%, which was the proper range [4-6]. Even though a carbon mass balance is important in oxidation reaction to analyze the mass balance of overall products, in this study, more focus was emphasized in IPN product, rather than CO+CO_2 values.

$$\text{m-xylene conversion (\%)} = \frac{\text{moles of m-xylene converted}}{\text{moles of m-xylene in}} \times 100$$

$$\text{IPN/TN yield (\%)} = \frac{\text{moles of IPN/TN formed}}{\text{moles of m-xylene in}} \times 100$$

RESULTS AND DISCUSSION

1. Physicochemical Characterization of Catalysts

Surface area, pore volume and pore diameter of V_2O_5/γ-Al_2O_3 catalysts are presented by the variance of V_2O_5 loading amounts in Table 1. Highest surface area of 115 m^2/g was obtained at 5 wt% of V_2O_5 loading on γ-Al_2O_3, of which result is similar to the surface area of γ-Al_2O_3 as received, 122 m^2/g. This indicates that a small quantity of V_2O_5 up to 5 wt% loading did not affect much to reduce the existing surface area of pure γ-Al_2O_3. And the pore size distribution of V_2O_5/γ-Al_2O_3 was presented along with the amount of V_2O_5 in Fig. 1. Relatively greater decrease of surface area data, from 115 to 98 m^2/g, was obtained with increasing V_2O_5 loading quantity from 5 to 10 wt%. And milder decrease was observed in 15 and 20 wt% of V_2O_5 loading. We suspect that monolayer formation may be formed until V_2O_5 loading reached to 10 wt%. It was claimed that the surface area of catalyst decreases steeper with increasing the amount of catalyst loading until a monolayer is formed [9,26]. During the process of monolayer formation, V_2O_5 penetrates and covers the pores of the support and conclusively causes lower surface area and lower pore volume. There was a noticeable decrease from 0.56 cc to 0.45 cc on pore volume at loading amount between 10 wt% and 15 wt%, while small decreases were observed at 20 wt% loading. Despite that the highest number of pore diameter was obtained at 10 wt%

Table 1. BET surface area, pore volume and pore diameter for V_2O_5/γ-Al_2O_3 catalysts with different V_2O_5 loadings

V_2O_5 loading (wt%)	Surface srea (m^2/g)	Pore volume (cc/g)
5	115	0.57
10	98	0.56
15	87	0.47
20	83	0.45

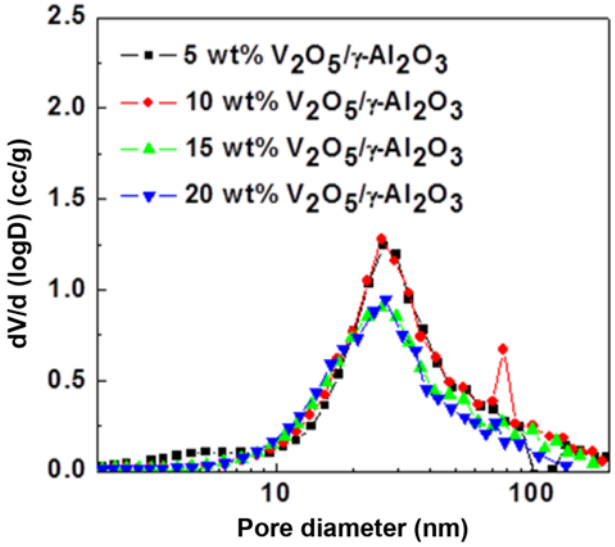

Fig. 1. Pore size distribution of V_2O_5/γ-Al_2O_3 catalysts with different V_2O_5 loadings.

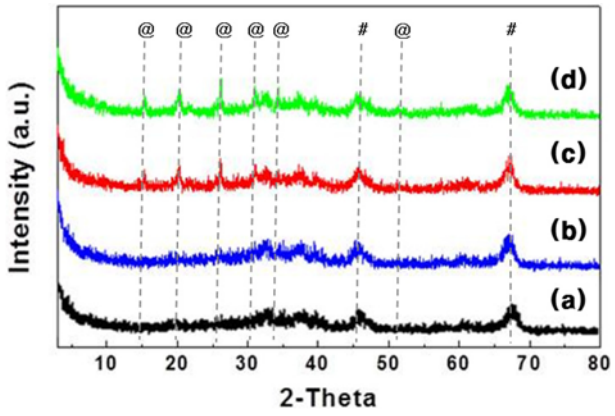

Fig. 2. XRD patterns of V_2O_5/Al_2O_3 catalysts with different V_2O_5 loadings (a) 5 wt% V_2O_5/γ-Al_2O_3, (b) 10 wt% V_2O_5/γ-Al_2O_3, (c) 15 wt% V_2O_5/γ-Al_2O_3 (d) 20 wt% V_2O_5/γ-Al_2O_3 : V_2O_5 (@); γ-Al_2O_3 (#).

of V_2O_5 loading, there were no significant differences in pore diameter at the range of 20 nm to 23 nm as shown in Fig. 3 [9,26].

Crystallographic change of V_2O_5/γ-Al_2O_3 was examined by XRD in variance of V_2O_5 loading amount and presented in Fig. 2. Crystalline peaks of V_2O_5 are assigned at 15.4, 20.37, 26.2, 31.08, 34.36 and 51.33 with respect to the value of 2-theta [26]. XRD patterns showed no crystallographic evidence of V_2O_5 up to 10 wt% of V_2O_5 loading. However, characteristic crystalline peaks of V_2O_5 were detected at both 15 wt% and 20 wt% of V_2O_5 loadings. We interpret that the catalysts with 5 wt% and 10 wt% loading are highly dispersed on the support because only characteristic XRD patterns of γ-Al_2O_3 were observed without characteristic XRD peaks of V_2O_5. At 15 wt% and 20 wt% V_2O_5 loadings, the V_2O_5 crystal peaks were clearly demonstrated, supporting the idea that bulk V_2O_5 crystallites were generated and V_2O_5 deposit coverage may be slight but greater than one monolayer. In case that the monolayer coverage is exceeded by V_2O_5 supply, in general, the formation of bulk $(V_2O_5)_n$ crystallites occur and uniform V_2O_5 dispersion decreases rapidly

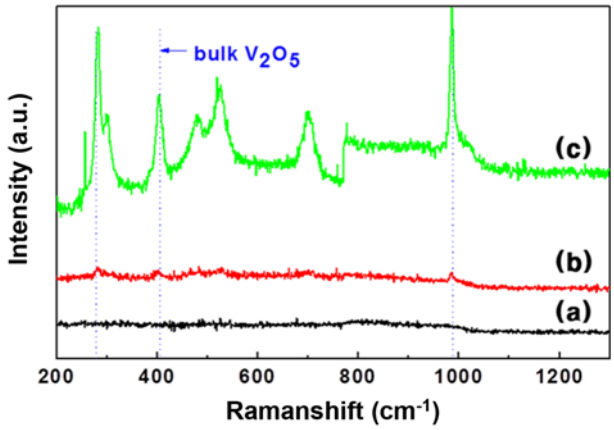

Fig. 3. Raman spectra of V_2O_5/γ-Al_2O_3 catalysts with different V_2O_5 loadings. (a) 5 wt% V_2O_5/γ-Al_2O_3, (b) 10 wt% V_2O_5/γ-Al_2O_3, (c) 15 wt% V_2O_5/γ-Al_2O_3.

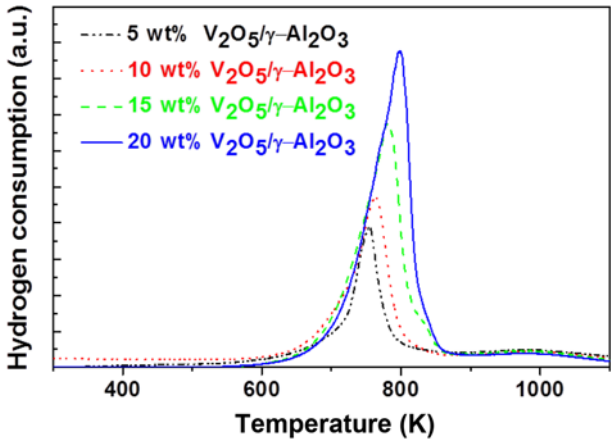

Fig. 4. Temperature-programmed reduction of V_2O_5/γ-Al_2O_3 catalysts with different V_2O_5 loadings.

[24,28].

Raman spectra of V_2O_5/γ-Al_2O_3 were collected at the wavelength range of 200-1,300 cm^{-1} and presented in Fig. 3. Samples include 5 wt%, 10 wt% and 15 wt% of V_2O_5 loadings. Characteristic Raman bands of V_2O_5 are observed at 988, 699, 527, 481, 401, 301 and 281 cm^{-1}, and each band corresponds to bulk V_2O_5 species [11,25, 27]. No significant Raman spectra were observed at 5 wt% of V_2O_5 loading, which may explain the high dispersion of V_2O_5 on γ-Al_2O_3. In case of 10 wt% of V_2O_5 loading, characteristic spectral peaks were generated at 988, 403, 281 cm^{-1}, but the peak intensities were hardly distinguishable with background noise, implying that monolayer formation may exist and early-stage bulk V_2O_5 crystals may start to grow [11]. Strong peak intensities were detected for 15 wt% of V_2O_5 loading at 991, 403 and 281 cm^{-1} which are of course the bulk V_2O_5 characteristic peaks as reported earlier [11]. Consistent with XRD interpretation, the monolayer of surface V_2O_5 species on γ-Al_2O_3 has been exceeded for over 15 wt% of V_2O_5 loading.

To evaluate the reduction performance of V_2O_5/γ-Al_2O_3 catalysts, TPR experiment was performed using H_2/Ar as reactants. The result is presented in Fig. 4. In literature, it has been reported that a sharp reduction peak is commonly found at 733-793 K [9,24]. The TPR

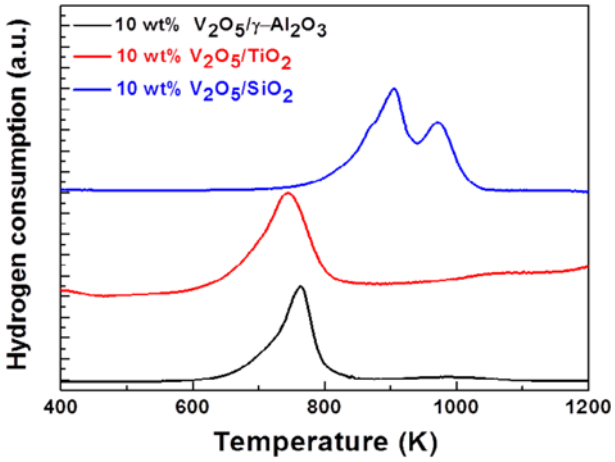

Fig. 5. Temperature-programmed reduction of V_2O_5 based catalysts with different supports.

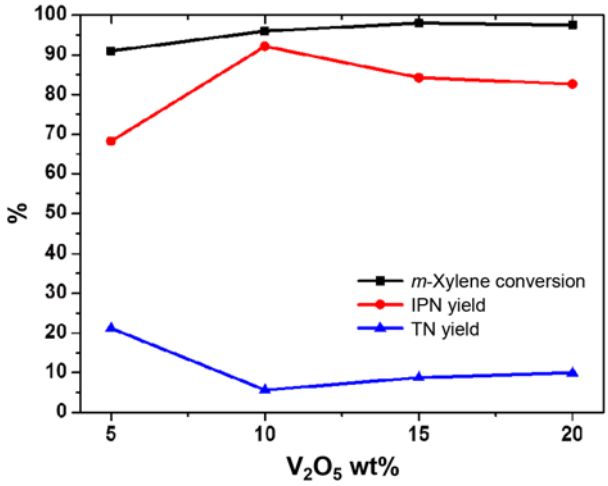

Fig. 6. Catalytic performance for ammoxidation of *m*-xylene on different V_2O_5 loadings.

data were recorded for the catalysts prepared with different V_2O_5 loadings on γ-Al_2O_3. The reduction behavior of the surface V_2O_5 species was observed in a strong dependency upon the quantity of V_2O_5 loading on γ-Al_2O_3. Observed were different reduction temperatures at 752 K for 5 wt%, 763 K for 10 wt%, 779 K for 15 wt% and 797 K for 20 wt% of V_2O_5 loadings, also shifted upward with increasing V_2O_5 loading amount. V_2O_5 would be reduced easier when it is dispersed in monolayer condition. Therefore, the lower reduction temperatures measured in 5 wt% and 10 wt% V_2O_5/γ-Al_2O_3 catalysts correspond to the higher dispersion of V_2O_5 on γ-Al_2O_3. In the literature, TPR peaks at above 773 K generally imply the presence of bulk V_2O_5 phases on support surface [9,24]. The reduction temperatures, 779 K for 15 wt% and 797 K for 20 wt% of V_2O_5 loadings, provided the clue that an increase of bulk V_2O_5 weakens dispersion degree and catalytic activity.

In Fig. 5, the TPR of the V_2O_5 based catalysts was also tested to investigate the reduction performance over different supports such as SiO_2, TiO_2 and γ-Al_2O_3. As different supports are employed, each reduction performance shows different tendency. A single reduction peak appeared at similar temperatures: 763 K for Al_2O_3 support and 756 K for TiO_2 support, respectively. Meanwhile, two reduction peaks were observed in case of SiO_2 support even at higher temperature. The lower peak position was interpreted by a better reduction performance. In other words, Al_2O_3 and TiO_2 supports seem more effective to produce a monolayer than SiO_2 support, and their lattice oxygen may participate more in the ammoxidation reaction.

2. Catalytic Activity for *m*-Xylene Ammoxidation

The test for *m*-xylene ammoxidation was conducted at a gas phase reaction system in order to minimize the formation of side products. In Fig. 6, the reactivity data of the catalyst with different V_2O_5 loadings on γ-Al_2O_3 support are summarized. Since IPN is the desired product from ammoxidation of *m*-xylene in this study, the selectivity and the yield of IPN and TN yield were calculated based on *m*-xylene conversion. The values in Fig. 5 show conversion increased gradually with increasingV_2O_5 loading amount.

As mentioned earlier, we interpret that 5 wt% and 10 wt% of V_2O_5 loading catalysts may have monolayer condition. Reported was that monolayer V_2O_5 species was more active and more selective than bulk V_2O_5 for the partial oxidation of hydrocarbons [27]. Even though monolayer condition existed at both 10 wt% and 5 wt% of loadings, better IPN yield occurred at 10 wt% of V_2O_5 loading with a low TN yield of 5.6%, which is considered as an intermediate. However, catalytic activity cannot be solely determined by V_2O_5 loading amount. In both cases of 15 wt% and 20 wt% of V_2O_5 loading samples, less yield of IPN and higher yield of TN behaviors were determined than 10 wt% of V_2O_5 loading in spite of superior conversions achieved. It is persuasive that bulk V_2O_5 phase may have less catalytic activity than monolayer V_2O_5. As a result, 10 wt% of V_2O_5 loading became the optimum monolayer capability for our experiment.

Table 2. Conversion of *m*-xylene, IPN yield and TN yield for V_2O_5 supported catalysts with different supports

Catalysts	Surface area (m^2/g)	*m*-Xylene conversion (%)	IPN yield (%)	TN yield (%)
10 wt% V_2O_5/TiO_2	41	84	48	35
10 wt% V_2O_5/SiO_2	232	89	38	46
10 wt% V_2O_5/γ-Al_2O_3	115	96	92	6

The effect of different oxide supports was examined by employing TiO_2 and SiO_2 individually. The reaction result is listed in Table 2. Fixed was V_2O_5 loading amount at 10 wt%. Noticeable difference in *m*-xylene conversion was observed. The *m*-xylene conversions were 84% for SiO_2, 89% for TiO_2 and 96% for γ-Al_2O_3. The IPN yields of V_2O_5/TiO_2 andV_2O_5/SiO_2 were 48% and 38%, respectively, which were much lower values than 92% for V_2O_5/Al_2O_5. As a result, V_2O_5/Al_2O_5 showed the greater performance than V_2O_5/TiO_2 and V_2O_5/SiO_2 when *m*-xylene ammoxidation was compared. V_2O_5 dispersion depends on the nature of maximum possible vanadium densities in different support lattice before bulk V_2O_5 formation on support surface [24,29,30]. It was introduced the vanadium density possibly placed of 5-10 #/nm^2 for γ-Al_2O_3, TiO_2 and ZrO_2 but just less than 1 #/nm^2 for the SiO_2 support [24,29,30]. This provides the idea that a higher density of V_2O_5 would induce a higher dispersion for

γ-Al_2O_3. Therefore, in case of SiO_2, least IPN yield was obtained even though the surface area of SiO_2 was very high because vanadium density on SiO_2 surface was very low (about 1 #/nm^2). The vanadium density is also related to the strength of the interaction between V_2O_5 and support oxides, which would be a predictable factor for V_2O_5 coverage and the nature of the support [9,27]. Meanwhile, V_2O_5/TiO_2 has a similar vanadium density and reduction performance but a lower surface area than V_2O_5/γ-Al_2O_3, which resulted in lower IPN yield (48 versus 92, shown in Table 2). The finding indicates that V_2O_5/γ-Al_2O_3 has the most support-V_2O_5 interaction and higher activity and higher selectivity than V_2O_5/TiO_2, V_2O_5/SiO_2 during *m*-xylene ammoxidation reaction.

CONCLUSIONS

Catalytic characteristics and performance of the V_2O_5/(support oxide) system were investigated by using various techniques and reaction experiment. Reactivity of catalysts was performed mainly in *m*-xylene ammoxidation. It is plausible that 5 wt% and 10 wt% V_2O_5 loading may be dispersed in monolayer condition, which was supported by XRD measurement and Raman spectra. V_2O_5/γ-Al_2O_3 showed the most effective conversion at 10 wt% of V_2O_5 loading. In case of higher content of V_2O_5 loading (15 wt% and 20 wt%), bulk V_2O_5 phase was formed and less IPN yield with higher TN yield was obtained during ammoxidation. The different behavior between monolayer V_2O_5 and bulk V_2O_5 was examined by TPR test. The dominant presence of V_2O_5 monolayer would be a crucial factor to increase the IPN selectivity and yield from direct ammoxidation of *m*-xylene. The theory about the maximum vanadium density was adapted to interpret why V_2O_5/γ-Al_2O_3 showed superior reactivity over V_2O_5/TiO_2 and V_2O_5/SiO_2.

ACKNOWLEDGEMENTS

This work was supported by the National Research Foundation of Korea (NRF) grant funded by the Korea government (MEST) (No. 2012R1A2A2A02011268).

REFERENCES

1. B. K. Hodnett and K. Hodnett, 1st Ed.,Wiley, New York (2000).
2. K. Weissermel, H.-J. Arpe, Vol. 3, Completelyrev. Ed., VCH, Weinheim (1997).
3. M. Amiridis, R. Duevel and I. E. Wachs, *Appl. Catal. B: Environ*., **23**, 111 (1999).
4. I. J. Lee, C. H. Lee, S. D. Lee and D. J. Suh, *J. Ind. Eng. Chem*., **11**, 918 (2005).
5. K. V. Narayana, A. Martin, U. Bentrup, B. Lücke and J. San, *Appl. Catal. A: Gen.*, **270**, 57 (2004).
6. M. Zhong, Y. G. Liang, Y Liu and Y. L. Ma, *Chem. Lett*., **34**, 646 (2005).
7. Y. Liu, M. Zhong, W. Yu and Y. L. Ma, *Syn. Comm*., **35**, 2951 (2005).
8. S. W. Row, T. Y. Chae, K. S. Yoo, S. D. Lee, D. W. Lee and Y. G. Shul, *Canadian J. Chem. Eng*., **85**, 925 (2007).
9. Ettireddy P. Reddy and Rajender S. Varma, *J. Catal*., **221**, 93 (2004).
10. L. Owens and H. H. Kung, *J. Catal*., **144**, 202 (1993).
11. M. A. Banares and I. E. Wachs, *J. Raman Spectrosc*., **33**, 359 (2002).
12. M. Ito, K. Sano and M. Kitabatake, *Adv. Chem.*, **76**, 288 (1968).
13. G. Y. Xie, Q. Zheng, C. Huang and Y. Y. Chen, *Ind. J. Chem*., **41A**, 963 (2002).
14. K. N. Rao, P. Venkataswamy, P. Bharali, H. Phil Ha and B. M. Reddy, *Res. Chem. Int*., **38**, 733 (2012).
15. C. L. Pieck, S. del Val, M. Lopez Granados, M. A. Banares and J. L. G. Fierro, *Langmuir*, **18**, 2642 (2002).
16. M. Niwa, H. Ando and Y. Murakami, *J. Catal*., **70**, 1 (1981).
17. H. P. Angstadt, M. C. H. Blackburn and R. Park, Sun Research & Development Co., US3845094 (1975).
18. D. R. Bushick and H. P. Angstadt, US 3,959,337 (1976).
19. M. Kenichi, M. Kunio and Y. Motoo, EP1452231A1 (2004).
20. K. R. Grasselli, *Catal. Today*, **49**, 141 (1999).
21. M. Sanatia, R. Akbari, S. Masetti and F. Triro, *Catal. Today*, **42**, 325 (1998).
22. K. V. Narayana, A. Venugopal, K. S. Rama Rao, V. Venkat Rao, S. Khaja Masthan and P. Kanta Rao, *Appl. Catal. A: Gen*., **150**, 269 (1997).
23. A. Martin and B. Lücke, *Catal. Today*, **57**, 61 (2000).
24. F. Klose, T. Wolff, H. Lorenz, A. Seidel-Morgenstern, Y. Suchorski, M. Piórkowska and H. Weiss, *J. Catal*., **247**, 176 (2007).
25. M. Brishti, E. W. Israel and D. Goutam, *J. Catal.*, **240**, 151 (2006).
26. I. Baldychev, R. J. Gorte and J. M. Vohs, *J. Catal*., 269, 397 (2010).
27. K. Routray, K. R. S. K. Reddy and Goutam Deo, *Appl. Catal. A: Gen*., **265**, 103 (2004).
28. S. T. Srinivas, L. Jhansi Lakshmi. P. S. Sai Prasad, S. S. Madhavendra and P. Kanta Rao, *J. Mater. Sci*., **32**, 965 (1997).
29. F. Arena, F. Fusteri and A. Parmaliana, *Appl. Catal. A: Gen.*, **176**, 189 (1999).
30. B. M. Reddy, E. P. Reddy, S. T. Srinivas, V. M. Mastikin, A. V. Nosov and O. B. Lapina, *J. Phys. Chem*., **96**, 7076 (1992).